FSU–HEP–940307

UCD–94–5

hep-ph/9403248

March 1994

Amplitude Zeros in $W^{\pm}Z$ Production

U. Baur

Department of Physics, Florida State University, Tallahassee, FL 32306, USA

T. Han and J. Ohnemus

Department of Physics, University of California, Davis, California 95616, USA

Abstract

We demonstrate that the Standard Model amplitude for $f_1\bar{f}_2 \to W^{\pm}Z$ at the Born-level exhibits an approximate zero located at $\cos\theta = (g_-^{f_1} + g_-^{f_2})/(g_-^{f_1} - g_-^{f_2})$ at high energies, where the $g_-^{f_i}$ $(i = 1, 2)$ are the left-handed couplings of the Z-boson to fermions and θ is the center of mass scattering angle of the W-boson. The approximate zero is the combined result of an exact zero in the dominant helicity amplitudes $\mathcal{M}(\pm, \mp)$ and strong gauge cancelations in the remaining amplitudes. For non-standard WWZ couplings these cancelations no longer occur and the approximate amplitude zero is eliminated.

Although the electroweak Standard Model (SM) based on an $\mathrm{SU_L}(2) \bigotimes \mathrm{U_Y}(1)$ gauge theory has been very successful in describing contemporary high energy physics experiments, the three vector-boson couplings predicted by this non-Abelian gauge theory remain largely untested experimentally. Careful studies of these couplings, for example in di-boson production in e^+e^- or hadronic collisions, may allow us not only to test the non-Abelian gauge structure of the SM [1], but also to explore new physics at higher mass scales [2].

The reaction $p\overset{(-)}{p} \to W^{\pm}\gamma$ is of special interest due to the presence of a zero in the amplitude of the parton-level subprocess $q_1\bar{q}_2 \to W^{\pm}\gamma$ at [3]

$$\cos\theta = \frac{Q_1 + Q_2}{Q_1 - Q_2} \,, \tag{1}$$

where θ is the scattering angle of the W-boson with respect to the quark (q_1) direction, and Q_i ($i = 1, 2$) are the quark charges in units of the proton electric charge e. This zero is a consequence of the factorizability [4] of the amplitudes in gauge theories into one factor which contains the gauge coupling dependence and another which contains spin information. Although the factorization holds for any four-particle Born-level amplitude in which one or more of the four particles is a gauge-field quantum, the amplitudes for most processes may not necessarily develop a kinematical zero in the physical region. The amplitude zero in the $W^{\pm}\gamma$ process has been further shown to correspond to the absence of dipole radiation by colliding particles with the same charge-to-mass ratio [5], a realization of classical radiation interference. This phenomenon may make it possible to measure the magnetic dipole moment and electric quadrupole moment of the W-boson [6,7].

In this Letter we study in detail the helicity amplitudes of the analogous process

$$f_1(p_1)\, \bar{f}_2(p_2) \to W(p_{\mathrm{w}})\, Z(p_{\mathrm{z}}) \,, \tag{2}$$

where f_i represents a quark or lepton and p_i denotes the particle four-momentum. The three lowest order Feynman diagrams contributing to the process $f_1\bar{f}_2 \to WZ$ are shown in Fig. 1. The helicity amplitudes for this process can be written as

$$\mathcal{M}(\lambda_{\mathrm{w}}, \lambda_{\mathrm{z}}) = F\, \epsilon^*_{\mu}(p_{\mathrm{w}}, \lambda_{\mathrm{w}})\, \epsilon^*_{\nu}(p_{\mathrm{z}}, \lambda_{\mathrm{z}})\, \overline{V}(p_2)\, T^{\mu\nu}\, \frac{1}{2}\,(1 - \gamma_5)\, U(p_1) \,, \tag{3}$$

where $\lambda_{\rm w}$ ($\lambda_{\rm z}$) denotes the W (Z) boson polarization ($\lambda = \pm 1, 0$ for transverse and longitudinal polarizations, respectively), ϵ denotes the weak-boson polarization vector, and U (V) represents the fermion (anti-fermion) spinor. The factor F contains coupling factors,

$$F = C\,\frac{e^2}{\sqrt{2}\sin\theta_{\rm w}}\,, \tag{4}$$

where $\theta_{\rm w}$ is the weak mixing angle, and C is a color factor; for leptons $C = 1$ and for quarks $C = \delta_{i_1 i_2}\,V_{f_1 f_2}$. Here i_1 (i_2) is the color index of the incoming quark (antiquark) and $V_{f_1 f_2}$ is the quark mixing matrix element. In the SM the tensor $T^{\mu\nu}$ is, in the limit of massless fermions,

$$T^{\mu\nu} = g_-^{f_1}\gamma^\mu\frac{(\not p_1 - \not p_{\rm z})}{u}\gamma^\nu + g_-^{f_2}\gamma^\nu\frac{(\not p_1 - \not p_{\rm w})}{t}\gamma^\mu + \frac{Q_W\,\cot\theta_{\rm w}}{s - M_W^2}\Big[(\not p_{\rm z} - \not p_{\rm w})\,g^{\mu\nu} + 2p_{\rm w}^\nu\gamma^\mu - 2p_{\rm z}^\mu\gamma^\nu\Big], \tag{5}$$

where the slash denotes a contraction with a Dirac gamma matrix, $\not p \equiv p_\mu\gamma^\mu$, M_W is the W-boson mass, Q_W is the electric charge of the outgoing W-boson, and $g_-^{f_i}$ are the couplings of the Z-boson to left-handed fermions:

$$g_-^f = \frac{1}{\sin\theta_{\rm w}\cos\theta_{\rm w}}\,(T_3^f - Q_f\sin^2\theta_{\rm w})\,. \tag{6}$$

In Eq. (6), $T_3^f = \pm\frac{1}{2}$ represents the third component of the weak isospin and Q_f is the electric charge of the fermion f. The kinematic variables are defined by

$$s = (p_1 + p_2)^2\,,\; t = (p_1 - p_{\rm w})^2 = -\frac{s}{2}\,(\alpha - \beta\cos\theta)\,,\; u = (p_1 - p_{\rm z})^2 = -\frac{s}{2}\,(\alpha + \beta\cos\theta)\,, \tag{7}$$

where

$$\alpha = 1 - r_{\rm w} - r_{\rm z}\,, \qquad \beta = (\alpha^2 - 4r_{\rm w}r_{\rm z})^{1/2}\,, \qquad r_{\rm v} = \frac{M_V^2}{s}\,, \tag{8}$$

with $V = W$, Z, and θ is the center of mass scattering angle of the W-boson with respect to the fermion (f_1) direction. In the SM, the $\mathrm{SU_L(2)}\bigotimes\mathrm{U_Y(1)}$ gauge structure relates the Z-boson to fermion couplings to the triple gauge-boson WWZ coupling by

$$g_-^{f_1} - g_-^{f_2} = Q_W\,\cot\theta_{\rm w}\,. \tag{9}$$

Using Eq. (9) and the kinematic identity $s+t+u = M_W^2 + M_Z^2$, the amplitude in Eq. (3) can be rewritten as

$$\mathcal{M}(\lambda_{\rm w},\lambda_{\rm z}) = \frac{F}{s}\,\overline{V}(p_2)\left[X\left(\not{A} - \frac{t}{s-M_W^2}\not{V}\right) + Y\not{V}\right](1-\gamma_5)\,U(p_1)\,, \tag{10}$$

where X and Y are combinations of coupling factors

$$X = \frac{s}{2}\left(\frac{g_-^{f_1}}{u} + \frac{g_-^{f_2}}{t}\right), \qquad Y = g_-^{f_1}\,\frac{M_Z^2\,s}{2\,u\,(s-M_W^2)}\,, \tag{11}$$

and

$$\not{A} = 2\,p_1{\cdot}\epsilon_{\rm w}^*\not{\epsilon}_{\rm z}^* + \not{\epsilon}_{\rm z}^*\not{\epsilon}_{\rm w}^*\not{p}_{\rm w}\,, \qquad \not{V} = 2\Big[\epsilon_{\rm w}^*{\cdot}\epsilon_{\rm z}^*\not{p}_{\rm z} + p_{\rm w}{\cdot}\epsilon_{\rm z}^*\not{\epsilon}_{\rm w}^* - p_{\rm z}{\cdot}\epsilon_{\rm w}^*\not{\epsilon}_{\rm z}^*\Big]\,, \tag{12}$$

contain the spin dependent parts. $\not{V}$ acts as a projection operator on the $J=1$ partial wave amplitudes. The form of the helicity amplitudes given in Eq. (10) is very convenient for studying the factorization properties of the WZ production amplitudes and for comparing with the helicity amplitudes for $q_1\bar{q}_2 \to W\gamma$. It is obvious that without the term Y, which is proportional to M_Z^2, the helicity amplitudes would factorize. In this case all amplitudes would simultaneously vanish for $g_-^{f_1}/u + g_-^{f_2}/t = 0$, in analogy to the $W\gamma$ case.

Further insight can be obtained from the explicit expressions for the helicity amplitudes $\mathcal{M}(\lambda_{\rm w},\lambda_{\rm z})$. Working in the parton center of mass frame, Eq. (10) yields

$$\mathcal{M}(\pm,\mp) = F\,\sin\theta\,\Big(\lambda_{\rm w} - \cos\theta\Big)X\,, \tag{13}$$

$$\mathcal{M}(\pm,\pm) = F\,\sin\theta\,\left[\left(\lambda_{\rm w}(r_{\rm z}-r_{\rm w}) - \beta + \cos\theta + \beta\,\frac{\alpha-\beta\cos\theta}{1-r_{\rm w}}\right)X + 2\beta Y\right]\,, \tag{14}$$

$$\mathcal{M}(0,0) = F\,\frac{\sin\theta}{\sqrt{2r_{\rm w}}2r_{\rm z}}\,\left[\left(-\beta\rho + \beta_{\rm w}\beta_{\rm z}\cos\theta + \beta\rho\,\frac{\alpha-\beta\cos\theta}{1-r_{\rm w}}\right)X + 2\beta\rho Y\right]\,, \tag{15}$$

$$\mathcal{M}(\pm,0) = F\,\frac{(1-\lambda_{\rm w}\cos\theta)}{\sqrt{2r_{\rm z}}}\,\left[\left(2\lambda_{\rm w}r_{\rm z} - \beta + \beta_{\rm z}\cos\theta + \beta\,\frac{\alpha-\beta\cos\theta}{1-r_{\rm w}}\right)X + 2\beta Y\right]\,, \tag{16}$$

$$\mathcal{M}(0,\pm) = F\,\frac{(1+\lambda_{\rm z}\cos\theta)}{\sqrt{2r_{\rm w}}}\,\left[\left(-2\lambda_{\rm z}r_{\rm w} - \beta + \beta_{\rm w}\cos\theta + \beta\,\frac{\alpha-\beta\cos\theta}{1-r_{\rm w}}\right)X + 2\beta Y\right]\,, \tag{17}$$

where $\beta_{\rm w}$, $\beta_{\rm z}$, and ρ are combinations of the kinematic invariants,

$$\beta_{\rm w} = 1 + r_{\rm w} - r_{\rm z}\,, \qquad \beta_{\rm z} = 1 - r_{\rm w} + r_{\rm z}\,, \qquad \rho = 1 + r_{\rm w} + r_{\rm z}\,. \tag{18}$$

The amplitudes given in Eqs. (13) – (17) contain the main results of our paper. They exhibit several interesting features. $\mathcal{M}(\pm,\mp)$ receive contributions only from $J \geq 2$ partial waves, *i.e.*, only from the u and t-channel fermion-exchange diagrams (see Fig. 1a and b). The $(\pm,\mp)$ amplitudes therefore do not depend on Y and thus factorize. They vanish for

$$\frac{g_-^{f_1}}{u} + \frac{g_-^{f_2}}{t} = 0\,, \qquad \text{or} \qquad \cos\theta_0 = \frac{\alpha}{\beta}\left(\frac{g_-^{f_1} + g_-^{f_2}}{g_-^{f_1} - g_-^{f_2}}\right)\,. \tag{19}$$

The existence of the zero in $\mathcal{M}(\pm,\mp)$ at $\cos\theta_0$ is a direct consequence of the contributing Feynman diagrams and the left-handed coupling of the W-boson to fermions. Unlike the $W^\pm\gamma$ case with its massless photon kinematics, the zero has an energy dependence through α and β which is, however, rather weak for energies sufficiently above the WZ mass threshold. More explicitly, for $s \gg M_V^2$, the zero is located at

$$\cos\theta_0 \simeq \begin{cases} \frac{1}{3}\tan^2\theta_{\rm w} \simeq 0.1 & \text{for } d\bar{u} \to W^-Z\,, \\ -\tan^2\theta_{\rm w} \simeq -0.3 & \text{for } e^-\bar{\nu}_e \to W^-Z\,, \\ -\frac{1}{3}\tan^2\theta_{\rm w} \simeq -0.1 & \text{for } u\bar{d} \to W^+Z\,, \\ \tan^2\theta_{\rm w} \simeq 0.3 & \text{for } \nu_e e^+ \to W^+Z\,. \end{cases}$$

At high energies, $s \gg M_V^2$, strong cancelations occur between the various terms in the square brackets in Eqs. (14) – (17) and only the $(\pm,\mp)$ and $(0,0)$ amplitudes remain non-zero:

$$\mathcal{M}(\pm,\mp) \longrightarrow \frac{F}{\sin\theta}\,(\lambda_{\rm w} - \cos\theta)\left[(g_-^{f_1} - g_-^{f_2})\cos\theta - (g_-^{f_1} + g_-^{f_2})\right]\,, \tag{20}$$

$$\mathcal{M}(0,0) \longrightarrow \frac{F}{2}\,\sin\theta\,\frac{M_Z}{M_W}\,(g_-^{f_2} - g_-^{f_1})\,. \tag{21}$$

Note that the amplitudes do not fully factorize in the high energy limit due to the survival of $\mathcal{M}(0,0)$. Because the Y term in Eq. (10) behaves like $(M_Z^2/s)\,\epsilon_{\rm w}^*\epsilon_{\rm z}^*$ at high energies, one might naively expect that the amplitudes completely factorize for $s \gg M_V^2$ as in the $W\gamma$ case. However, for longitudinally polarized vector bosons $\epsilon_{\rm v}^* \sim \sqrt{s}/M_V$ and thus the $(0,0)$ amplitude remains finite.

The combined effect of the zero in $\mathcal{M}(\pm,\mp)$ and the gauge cancelations at high energies in the remaining helicity amplitudes results in an approximate zero for the $f_1\bar{f}_2 \to W^\pm Z$ differential cross section at $\cos\theta \approx \cos\theta_0$. This is illustrated in Fig. 2 where we show the differential cross sections for $e^-\bar{\nu}_e \to W^-Z$ and $d\bar{u} \to W^-Z$,

$$\frac{d\sigma(\lambda_{\rm w},\lambda_{\rm z})}{d\cos\theta} = \frac{\beta}{32\pi s}\,\overline{|\mathcal{M}(\lambda_{\rm w},\lambda_{\rm z})|^2}\,, \tag{22}$$

(the over-line denotes the fermion-spin and color averaged squared matrix element) for $(\lambda_{\rm w},\lambda_{\rm z}) = (\pm,\mp)$ and $(0,0)$, as well as the unpolarized cross section, which is obtained by summing over all W- and Z-boson helicity combinations (solid line). Although the matrix elements are calculated at $\sqrt{s} = 2$ TeV, the results differ little from those obtained in the high energy limit. For both reactions, the total differential cross section displays a pronounced minimum at the location of the zero in $\mathcal{M}(\pm,\mp)$. Due to the $1/\sin\theta$ behaviour of $\mathcal{M}(\pm,\mp)$, the $(+,-)$ and $(-,+)$ amplitudes dominate outside of the region of the zero. In order to demonstrate the influence of the zero in $\mathcal{M}(\pm,\mp)$ on the total angular differential cross section, we have included the $\cos\theta$ distribution for $e^+e^- \to ZZ$ in Fig. 2a, normalized to the $e^-\bar{\nu}_e \to W^-Z$ cross section at $\cos\theta = 0.9$ (long dashed line). The zero in the $(\pm,\mp)$ amplitudes causes the minimum in the WZ case to be much more pronounced than the minimum in $e^+e^- \to ZZ$.

Figure 3 illustrates the energy dependence of the differential cross section. At $\sqrt{s} =$ 0.2 TeV, *i.e.* close to the threshold, contributions from the $(\pm,\pm)$, $(\pm,0)$, and $(0,\pm)$ amplitudes are all important. These amplitudes do not factorize in terms of X and therefore tend to eliminate the approximate zero (dotted lines). Above threshold, these contributions rapidly diminish, as exemplified by the curves for $\sqrt{s} = 0.5$ TeV (dashed lines) and $\sqrt{s} = 2$ TeV (solid lines). Note that the location of the minimum varies only slightly with energy.

The results obtained so far demonstrate that the SM WZ cross section exhibits an approximate kinematical zero in the physical region in the high energy limit. This behavior is due to the combined effect of an exact zero in $\mathcal{M}(\pm,\mp)$ and strong cancelations in the

remaining amplitudes. Non-standard WWZ couplings spoil these cancelations and eliminate the approximate zero. To illustrate this, we consider the general C and P conserving effective Lagrangian [1]

$$\mathcal{L}_{WWZ} = -i\, e \cot\theta_{\rm w} \left[g_1 \left(W^\dagger_{\mu\nu} W^\mu Z^\nu - W^\dagger_\mu Z_\nu W^{\mu\nu} \right) + \kappa\, W^\dagger_\mu W_\nu Z^{\mu\nu} + \frac{\lambda}{M_W^2}\, W^\dagger_{\lambda\mu} W^\mu_\nu Z^{\nu\lambda} \right] , \quad (23)$$

where W^μ and Z^μ are the W^- and Z fields, respectively, and $V_{\mu\nu} = \partial_\mu V_\nu - \partial_\nu V_\mu$, $V = W,\, Z$. In the SM at tree level, $g_1 = 1$, $\kappa = 1$, and $\lambda = 0$. The contributions to the WZ production amplitudes from the anomalous couplings $\Delta g_1 = g_1 - 1$, $\Delta\kappa = \kappa - 1$, and λ are

$$\Delta\mathcal{M}(\pm,\mp) = 0\,, \quad (24)$$

$$\Delta\mathcal{M}(\pm,\pm) = \frac{F}{2}\, \frac{Q_W\, \cot\theta_{\rm w}}{1 - r_{\rm w}}\, \beta \sin\theta \left[\Delta g_1 + \Delta\kappa + \frac{\lambda}{r_{\rm w}} \right] , \quad (25)$$

$$\Delta\mathcal{M}(0,0) = \frac{F}{2}\, \frac{Q_W\, \cot\theta_{\rm w}}{1 - r_{\rm w}}\, \frac{\beta \sin\theta}{\sqrt{2r_{\rm w} 2r_{\rm z}}}\, 2 \left[\Delta g_1 (1 + r_{\rm w}) + \Delta\kappa\, r_{\rm z} \right] , \quad (26)$$

$$\Delta\mathcal{M}(\pm,0) = \frac{F}{2}\, \frac{Q_W\, \cot\theta_{\rm w}}{1 - r_{\rm w}}\, \frac{\beta(1 - \lambda_{\rm w} \cos\theta)}{\sqrt{2r_{\rm z}}} \left[2\,\Delta g_1 + \lambda\, \frac{r_{\rm z}}{r_{\rm w}} \right] , \quad (27)$$

$$\Delta\mathcal{M}(0,\pm) = \frac{F}{2}\, \frac{Q_W\, \cot\theta_{\rm w}}{1 - r_{\rm w}}\, \frac{\beta(1 + \lambda_{\rm z} \cos\theta)}{\sqrt{2r_{\rm w}}} \left[\Delta g_1 + \Delta\kappa + \lambda \right] . \quad (28)$$

The amplitudes given in Eqs. (24) – (28) agree with those of Refs. [8] apart from terms proportional to $(M_Z^2 - M_W^2)/s$ in $\Delta\mathcal{M}(0,0)$. The expression given in Eq. (26) corrects a minor error in Ref. [8].

Due to angular momentum conservation, the $(\pm,\mp)$ amplitudes which dominate in the SM do not receive any contributions from the anomalous couplings. The amplitude zero in these channels thus remains exact. All other helicity amplitudes are modified in the presence of non-standard WWZ couplings. At high energies the anomalous contributions grow proportional to $\sqrt{s}$ (s) for $\Delta\kappa$ (Δg_1 and λ) and thus could dominate the cross section. λ, Δg_1, and $\Delta\kappa$ contribute predominantly to the $(\pm,\pm)$, $(0,0)$, and $(0,\pm)$ amplitudes, respectively [9]. The influence of non-standard WWZ couplings on the differential cross section is illustrated in Fig. 4, where we compare $d\sigma/d\cos\theta$ for $d\bar{u} \to W^-Z$ at $\sqrt{s} = 500$ GeV for $\lambda = 0.1$, $\Delta g_1 = 0.2$, and $\Delta\kappa = 0.5$ (solid lines) with the SM result (dashed lines).

Besides the total cross section, we also display the cross section for the helicity state which produces the largest non-standard contribution for the given anomalous coupling. In each case displayed, the approximate zero present in the SM is completely eliminated by the anomalous coupling.

We finally comment briefly on observable signals of the approximate zero in WZ production in the SM. $e\nu_e$ or $\mu\nu_\mu$ collisions above the WZ threshold would in principle provide a clean environment, and the location of the zero at $\cos\theta_0 \approx \pm 0.3$ is ideal for experimental studies of the $W^\pm Z$ final state, unlike the case for $e^-\bar{\nu}_e \to W^-\gamma$ where the zero is located at the kinematical boundary, $\cos\theta = 1$ [3]. In the foreseeable future WZ production can be studied most easily in hadronic collisions. Since the high energy limit of the helicity amplitudes is approached very rapidly above threshold, the approximate amplitude zero in the SM results in a dip in the distribution of the Z-boson rapidity in the parton center of mass frame in $p\overset{(-)}{p} \to WZ$, in complete analogy to the dip in the photon center of mass rapidity distribution which signals the radiation zero in $W\gamma$ production [7]. Alternatively, one can study W-Z rapidity correlations where a similar dip occurs [10].

In summary, we have demonstrated that the amplitude for $f_1\bar{f}_2 \to W^\pm Z$ at Born-level exhibits an approximate zero in the SM in the physical region at high energies. The approximate zero is the combined result of an exact zero in $\mathcal{M}(\pm,\mp)$ and strong gauge cancelations in the remaining helicity amplitudes. The zero in the $(\pm,\mp)$ amplitudes is a direct consequence of the contributing Feynman diagrams and the left-handed coupling of the W-boson to fermions. Anomalous WWZ couplings spoil the gauge cancelations and eliminate the effect. The approximate amplitude zero leads to a pronounced dip in the Z-boson center of mass rapidity distribution in $p\overset{(-)}{p} \to WZ$, which in principle can be observed experimentally.

ACKNOWLEDGMENTS

We would like to thank T. Fuess, C. Wendt, and D. Zeppenfeld for stimulating discussions. This work has been supported in part by Department of Energy grants #DE-FG03-91ER40674 and #DE-FG05-87ER40319 and by Texas National Research Laboratory grant #RGFY93-330. T.H. is also supported in part by a UC-Davis Faculty Research Grant.

REFERENCES

[1] K. Gaemers and G. Gounaris, Z. Phys. **C 1**, 259 (1979); K. Hagiwara, R. D. Peccei, D. Zeppenfeld, and K. Hikasa, Nucl. Phys. **B 282**, 253 (1987).

[2] A. De Rujula *et al.*, Nucl. Phys. **B 384**, 3 (1992); A. Falk, M. Luke, and E. Simmons, Nucl. Phys. **B 365**, 523 (1991); J. Bagger, S. Dawson, and G. Valencia, Nucl. Phys. **B 399**, 364 (1993); K. Hagiwara *et al.*, Phys. Rev. **D 48**, 2182 (1993); C. Burgess and D. London, Phys. Rev. **D 48**, 4337 (1993); C. Arzt, M. B. Einhorn, and J. Wudka, Phys. Rev. **D 49**, 1370 (1994).

[3] R. W. Brown, K. O. Mikaelian, and D. Sahdev, Phys. Rev. **D 20**, 1164 (1979); K. O. Mikaelian, M. A. Samuel, and D. Sahdev, Phys. Rev. Lett. **43**, 746 (1979).

[4] D. Zhu, Phys. Rev. **D 22**, 2266 (1980); C. J. Goebel, F. Halzen, and J. P. Leveille, Phys. Rev. **D 23**, 2682 (1981).

[5] S. J. Brodsky and R. W. Brown, Phys. Rev. Lett. **49**, 966 (1982); R. W. Brown, K. L. Kowalski, and S. J. Brodsky, Phys. Rev. **D 28**, 624 (1983); R. W. Brown and K. L. Kowalski, Phys. Rev. **D 29**, 2100 (1984).

[6] G. N. Valenzuela and J. Smith, Phys. Rev. **D 31**, 2787 (1985); J. Cortes, K. Hagiwara, and F. Herzog, Nucl. Phys. **B 278**, 26 (1986).

[7] U. Baur and D. Zeppenfeld, Nucl. Phys. **B 308**, 127 (1988).

[8] U. Baur and D. Zeppenfeld, Phys. Lett. **B 201**, 383 (1988); K. Hagiwara, J. Woodside, and D. Zeppenfeld, Phys. Rev. **D 41**, 2113 (1990).

[9] D. Zeppenfeld and S. S. D. Willenbrock, Phys. Rev. **D 37**, 1775 (1988).

[10] S. Frixione, P. Nason, and G. Ridolfi, Nucl. Phys. **B 383**, 3 (1992).

FIGURES

FIG. 1. Feynman diagrams contributing to the Born-level subprocess $f_1\bar{f}_2 \to WZ$.

FIG. 2. Differential cross section $d\sigma(\lambda_{\rm w},\lambda_{\rm z})/d\cos\theta$ versus the W^- scattering angle θ in the center of mass frame for the Born-level processes (a) $e^-\bar{\nu}_e \to W^-Z$ and (b) $d\bar{u} \to W^-Z$. The dashed, dotted, and dash-dotted curves are for $(\lambda_{\rm w},\lambda_{\rm z}) = (0,0)$, $(+,-)$, and $(-,+)$, respectively. The solid line represents the total (unpolarized) cross section. For comparison, the long dashed curve in (a) shows the $e^+e^- \to ZZ$ cross section, normalized to the $e^-\bar{\nu}_e \to W^-Z$ cross section at $\cos\theta = 0.9$.

FIG. 3. Differential cross section $d\sigma/d\cos\theta$ versus the W^- scattering angle θ in the center of mass frame for the Born-level processes (a) $e^-\bar{\nu}_e \to W^-Z$ and (b) $d\bar{u} \to W^-Z$. The dotted, dashed, and solid curves are for $\sqrt{s} = 0.2$, 0.5, and 2 TeV, respectively.

FIG. 4. Differential cross sections for the subprocess $d\bar{u} \to W^-Z$ at $\sqrt{s} = 500$ GeV with anomalous couplings as defined in Eq. (23). Parts a), b), and c) are for $\lambda = 0.1$, $\Delta g_1 = 0.2$, and $\Delta\kappa = 0.5$, respectively. The solid (dashed) lines give the total differential cross section with (without) anomalous WWZ couplings. The dotted curves show the cross section for the helicity state which produces the largest non-standard contribution for the given anomalous coupling.

This figure "fig1-1.png" is available in "png" format from:

http://arXiv.org/ps/hep-ph/9403248v1

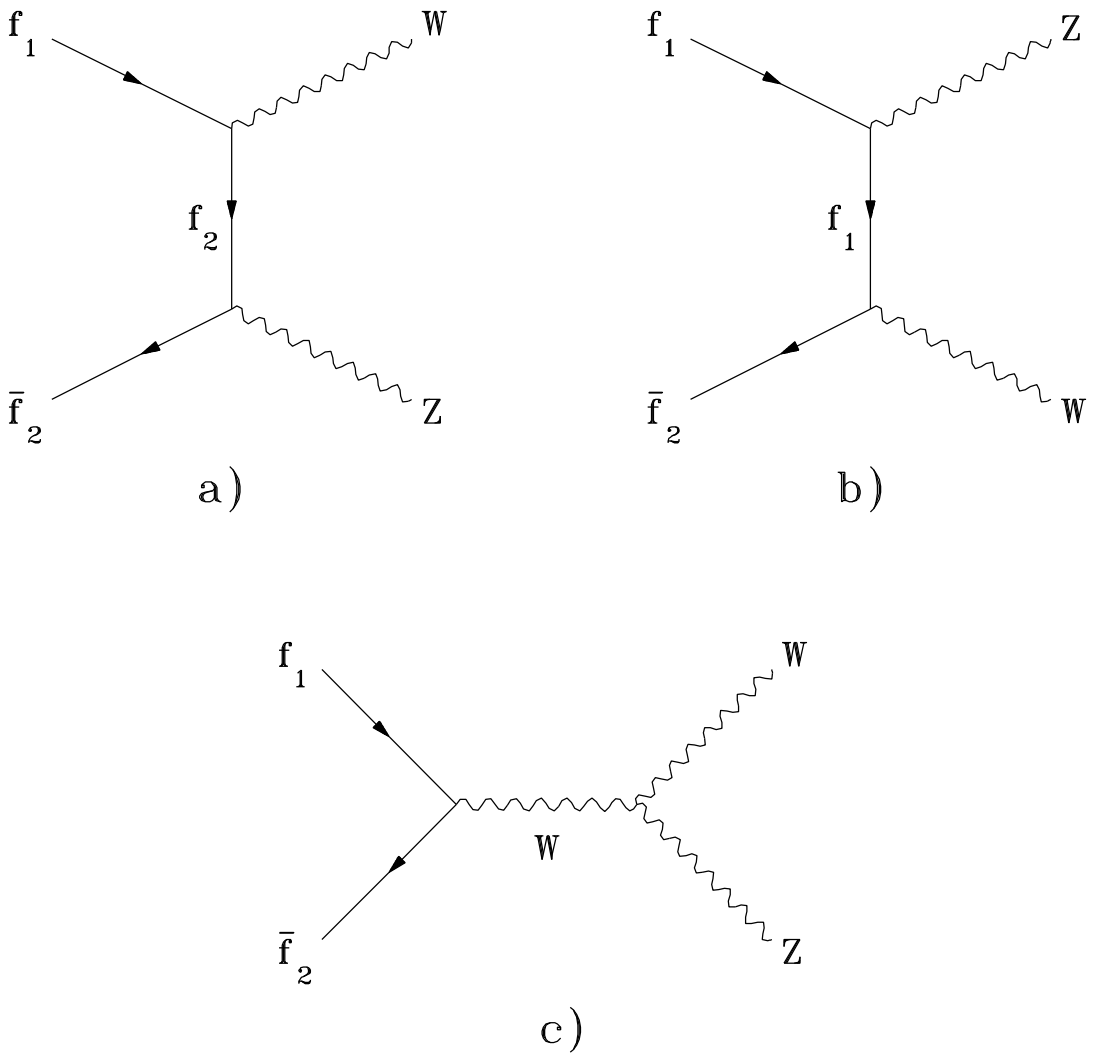

Figure 1

This figure "fig1-2.png" is available in "png" format from:

http://arXiv.org/ps/hep-ph/9403248v1

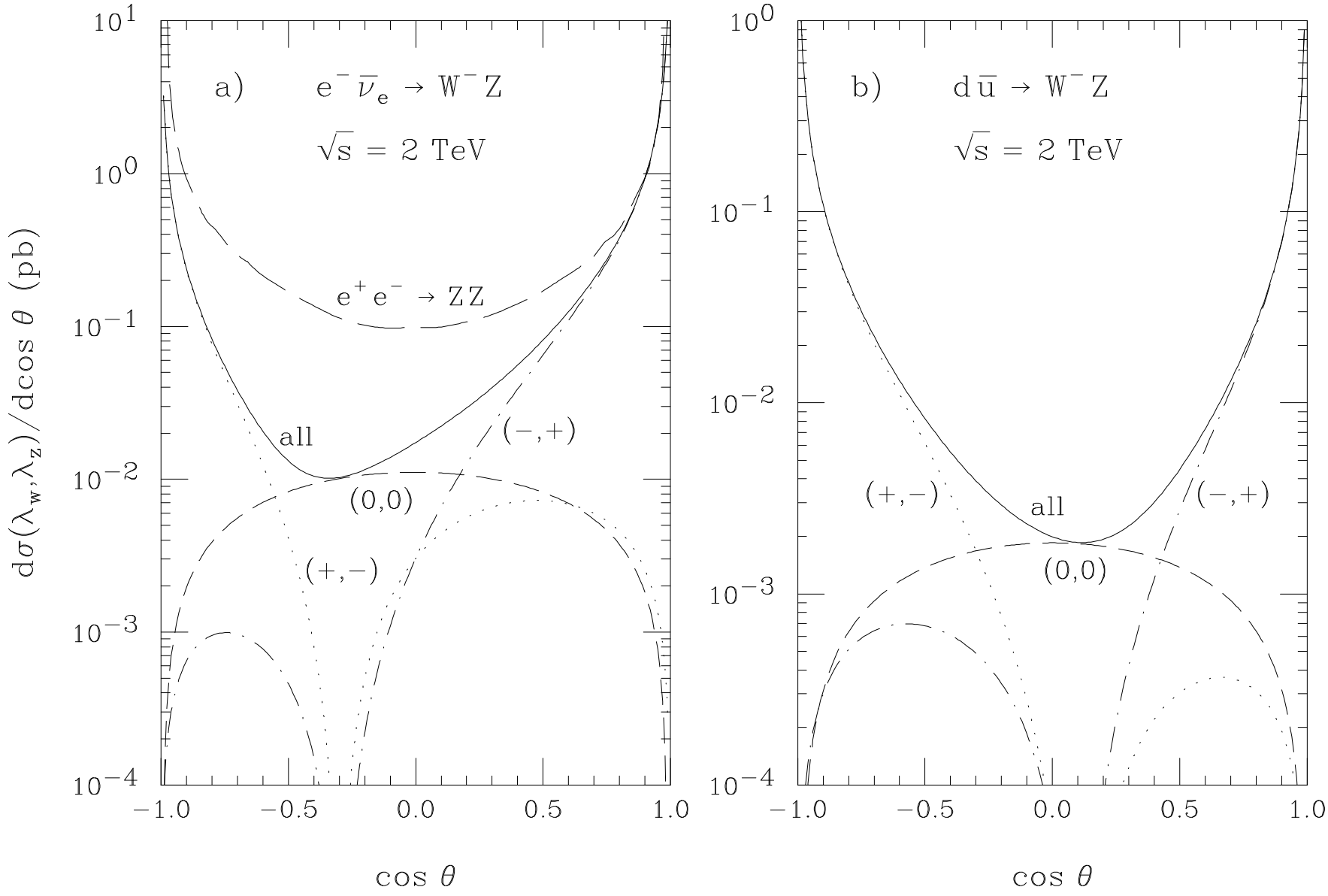
a)
$e^- \bar{\nu}_e \to W^- Z$
$\sqrt{s}$ = 2 TeV
$e^+ e^- \to ZZ$
all
(0,0)
(+,−)
(−,+)
b)
$d \bar{u} \to W^- Z$
$\sqrt{s}$ = 2 TeV
(+,−)
all
(0,0)
(−,+)
$d\sigma(\lambda_W,\lambda_Z)/d\cos\theta$ (pb)
cos θ
cos θ

Figure 2

This figure "fig1-3.png" is available in "png" format from:

http://arXiv.org/ps/hep-ph/9403248v1

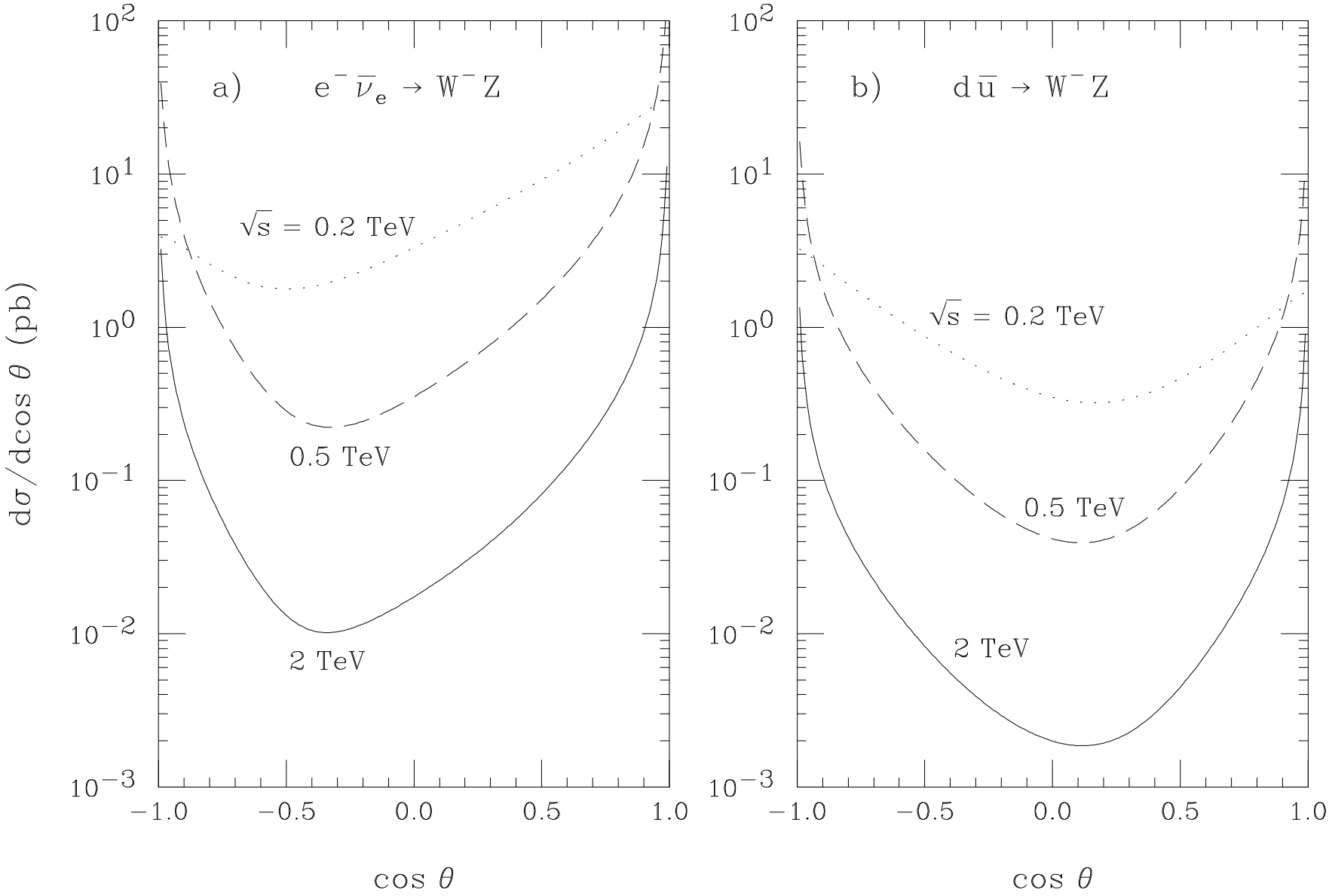
a) $e^- \bar{\nu}_e \to W^- Z$
b) $d \bar{u} \to W^- Z$
$\sqrt{s}$ = 0.2 TeV
0.5 TeV
2 TeV
$d\sigma/d\cos\theta$ (pb)
$\cos\theta$
10^2
10^1
10^0
10^{-1}
10^{-2}
10^{-3}
−1.0
−0.5
0.0
0.5
1.0

Figure 3

This figure "fig1-4.png" is available in "png" format from:

http://arXiv.org/ps/hep-ph/9403248v1

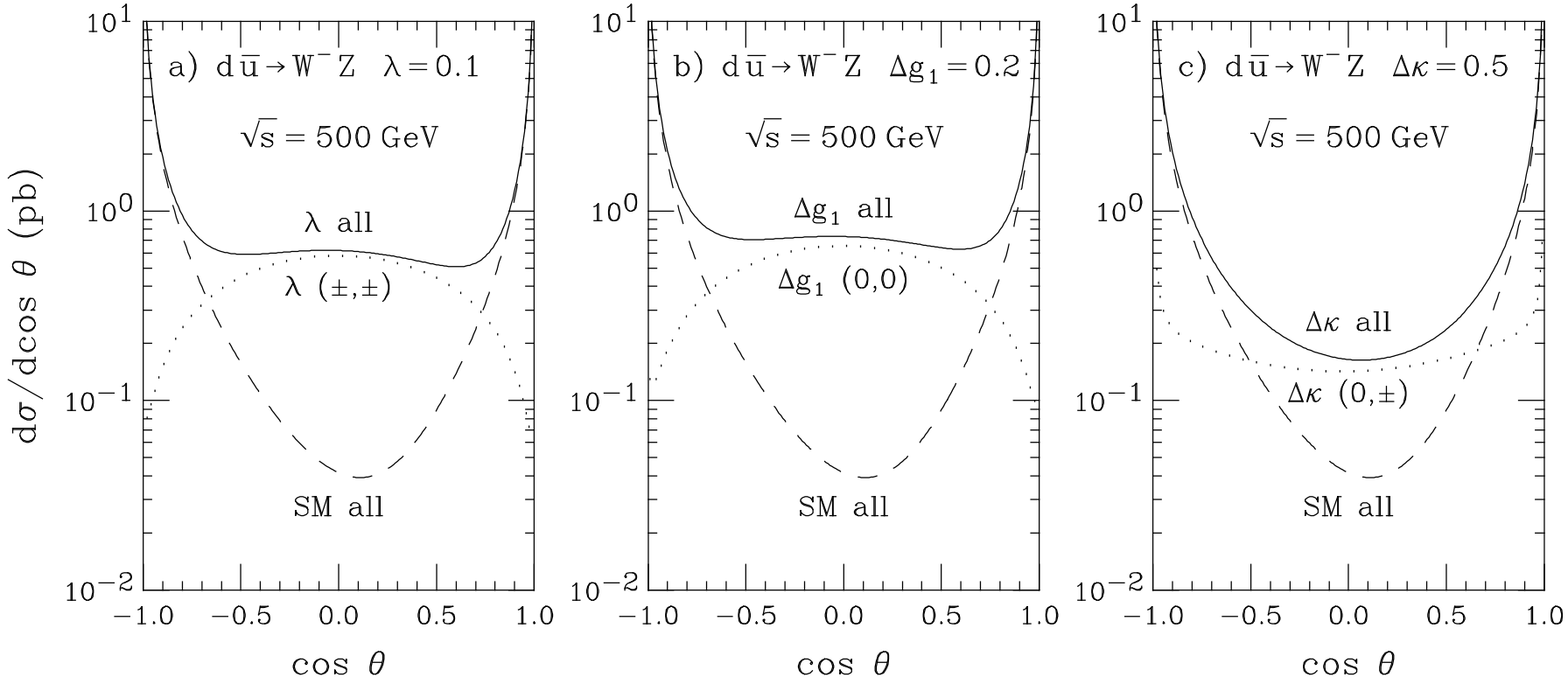
a) d ū → W⁻ Z λ = 0.1
√s = 500 GeV
λ all
λ (±,±)
SM all
b) d ū → W⁻ Z Δg1 = 0.2
√s = 500 GeV
Δg1 all
Δg1 (0,0)
SM all
c) d ū → W⁻ Z Δκ = 0.5
√s = 500 GeV
Δκ all
Δκ (0,±)
SM all
dσ/dcos θ (pb)
cos θ
10¹
10⁰
10⁻¹
10⁻²
−1.0
−0.5
0.0
0.5
1.0

Figure 4